Eur. Phys. J. D **32**, 19–24 (2005)
DOI: 10.1140/epjd/e2004-00150-y

THE EUROPEAN PHYSICAL JOURNAL D

Contribution of ion emission to sputtering of uranium dioxide by highly charged ions

Monomers and cluster size distributions

S. Boudjadar[a], F. Haranger, T. Jalowy, A. Robin, B. Ban d'Etat, T. Been, Ph. Boduch, H. Lebius, B. Manil, L. Maunoury, and H. Rothard[b]

Centre Interdisciplinaire de Recherche Ions Lasers CIRIL, UMR 6637 (CEA-CNRS-ENSICAEN), boulevard Henri Becquerel, 14070 Caen Cedex 05, France

Received 8 April 2004 / Received in final form 7 September 2004
Published online 3 November 2004 –

Abstract. Measurements of the cluster size (n) distribution of secondary $(UO_x)_n^+$ ions from sputtering of uranium dioxide (UO_2) by Ne^{8+}, Ar^{8+} and Xe^{q+} ions (q = 10, 23) at fixed kinetic energy (81 keV) have been performed with a time-of-flight mass spectrometer. The cluster ion yields Y follow a power law $Y(n) \sim n^{\delta}$ with $-2.1 < \delta < -1.5$. This is in contrast to a statistical recombination of the constituents upon ejection, but in agreement with the predictions of collective ejection models. Such a power law was also observed in the electronic stopping regime with MeV/u ions. The exponent δ is found to decrease with increasing projectile mass (and thus total sputter yield) at fixed kinetic energy. The ratio of emitted ionic clusters to monomers varies from 3 to 4.5 depending on the projectile. The contribution of positive ions to the total sputtering yield amounts to about 0.03%.

PACS. 34.50.Dy Interactions of atoms and molecules with surfaces; photon and electron emission; neutralization of ions – 79.20.-m Impact phenomena (including electron spectra and sputtering) – 61.80.Jh Ion radiation effects

1 Introduction

Nano-structuring of surfaces belongs to the most important topics in modern material research. Ion beams may induce nuclear tracks in solids and lead to surface modification. Therefore, favoured techniques in this field use ion beam structuring, whereas the energy transfer from the projectile to the target atoms and electrons leads to secondary particle emission, which are useful as probes of the dynamics of energy deposition. There are three different mechanisms contributing to the removal of target atoms from solid surfaces (sputtering): (a) elastic collisions with the target nuclei (nuclear energy loss), (b) inelastic collisions with the target electrons (electronic energy loss) and (c) (for highly charged ions) potential energy deposition. For reviews of sputtering, see e.g. [1–3], and references therein.

In the low energy regime (below the Bohr velocity $v_0 \approx 25$ keV/u) and for low primary charge states ($q \approx 1$), the nuclear stopping dominates. This regime is well described by the sputtering theory developed by Sigmund for linear collision cascades [2,4], although non-linear effects have to be accounted for in the case of high energy deposition [2,5]. In recent years, a great interest has arisen concerning the possible contribution of the potential energy release of slow highly charged ions (potential sputtering) [6,7]. While a slow ion with a high charge state approaches a surface, electronic capture from the solid to the projectile occurs. Therefore, in addition to projectile kinetic energy deposition (related to elastic and inelastic collisions) a strong localized electronic excitation is induced close to the surface. With high velocity projectiles (≈MeV/u) the electronic stopping dominates the projectile energy loss and may lead to electronic sputtering [2,3,8].

It is still an open question which mechanisms lead to electronic or potential sputtering depending on target material, ion charge and energy. Possible candidates include excitonic mechanisms [7,9], thermal spike [2,3,8,10] and Coulomb explosion [11], or combinations thereof. The basic understanding of the physical processes involved and the dynamics of the energy transfer to the target are essential for applications in nano-structuring of materials.

Sputtering of solids by ions may not only lead to the removal of single atoms, but also to the emission of stable, intact clusters from the surface [2,3,12–14]. The size

[a] *Permanent address:* LRPCSI, Université de Skikda, Route d'El-Hadaiek, B.P. 26, 21000 Skikda, Algeria.
[b] e-mail: `rothard@ganil.fr`

distribution of emitted cluster can be studied experimentally by measuring mass spectra of emitted particles. The techniques used [2,6] include time-of-flight (TOF) techniques for emitted ions [13] and LASER post-ionized neutrals [12]. Another technique is the analysis by transmission electron microscopy of emitted particles on a suitable collector [14].

The sputtering of uranium dioxide was studied at CIRIL-GANIL (Grand Accélérateur National d'Ions Lourds) both at high energy [15,16] in the electronic stopping power regime (≈MeV/u), and with low-energy highly charged ions (≈ q keV) [17,18]. Angular distributions and total sputter yields Y_{tot} of neutrals were measured by means of the catcher technique [15–18]. Such studies do not allow observing whether the material is sputtered as atoms, monomers, molecules or clusters. Therefore, we have extended these studies and now focus on the contribution of emitted $(UO_x)_n^+$ clusters ($n = 1 \ldots 7, x = 0 \ldots 3$) to sputtering of uranium dioxide UO_2, investigated by TOF mass spectroscopy.

2 Experiment

The experiment was performed at LIMBE ("Ligne d'Ions Multichargés de Basse Énergie"), GANIL's low energy multiply charged ion beam line [19]. Ne^{8+}, Ar^{8+} and Xe^{q+} ions ($q = 10, 23$) at a fixed kinetic energy of $E_{kin} = 81$ keV were used. This allows on the one hand, for a given fixed kinetic energy of 81 keV, to vary the potential energy E_{pot} of the projectile (defined as the sum of the ionization energies up to the corresponding charge state) from $E_{pot} \approx 0.8$ keV to $E_{pot} \approx 6.5$ keV with xenon ions of charge state $q = 10$ and $q = 23$, respectively. It is important to note that the potential energy of Xe^{10+} is comparable to (and in between) that of Ar^{8+} ($E_{pot} \approx 0.6$ keV) and Ne^{8+} ($E_{pot} \approx 0.9$ keV). Therefore, on the other hand, we also varied the projectile mass while keeping potential energy and kinetic energy constant.

In order to perform the experiment under conditions comparable to measurements of total sputter yields performed in our laboratory [17,18], the same procedures of target preparation were applied. The target is made from sintered powder of uranium dioxide UO_2 through cycling of mechanical polishing and annealing in reducing atmosphere (1400 °C, Ar/H_2). The surface quality (roughness and grain size distribution) is then controlled with AFM (Atomic Force Microscopy) ex situ. The stoichiometry was checked by X-ray diffraction, which showed that over a probing depth of ≈2 μm, only the UO_2 phase is present, and no traces of the U_3O_8 phase are detectable. The procedures are described in great detail in reference [17].

A sketch of the experimental set-up is shown in Figure 1. The experiment was performed in a mobile ultrahigh vacuum chamber designed for secondary particle emission studies at the different GANIL beam lines [20] in a vacuum of 5×10^{-8} mbar or better. A pulsed beam impinges on the uranium dioxide target with an incidence angle of 60° with respect to the surface normal. The emitted secondary ions are accelerated by a positive target

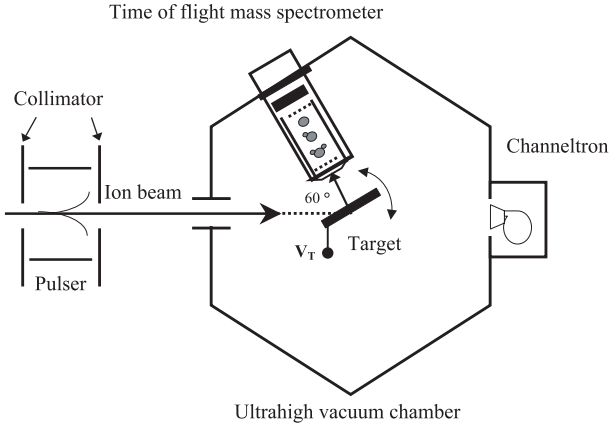

Fig. 1. Experimental set-up (see text).

extraction potential ($V_T \approx +500$ V $\ldots +1350$ V) towards a field-free drift tube. They are detected with a commercial secondary ion detector. The ions are post-accelerated (−2400 V) before hitting a dual microchannel plate (MCP). The extraction voltage is pulsed in order to avoid deflection of the pulsed slow ion beam. The ion beam is pulsed with a fast rising high voltage pulse applied to parallel deflection plates. The corresponding trigger pulse is used as a start signal, and the MCP pulse as stop signal for the measurement of the time-of-flight (TOF) of the secondary ions. This technique may be referred to as TOF-SIMS (Time of Flight-Secondary Ion Mass Spectroscopy) [4,11]. The beam pulse width, which determines the TOF and mass resolution, was measured with a channeltron detector, and found to be $\Delta t \approx 80$ ns.

An example for a time-of-flight spectrum induced by Xe^{23+} (81 keV) on UO_2 is shown in Figure 2a. Since the detection efficiency of the MCP detector decreases with increasing secondary ion mass (if the extraction and post acceleration potentials are held constant), we corrected the spectra accordingly [21,22]. Corrected and uncorrected spectra are compared in Figure 2a. The emission of $(UO_x)_n$ clusters up to a size of $n = 7$ can clearly be observed. From the mass spectra, cluster size distributions, i.e. the cluster yield $Y(n)$ as a function of the cluster size n can be derived. The mass resolution of our spectrometer does not allow to separate the individual contributions of U, UO, UO_2 and UO_3 to the peaks of the ionic clusters $(UO_x)_n^+$ for $n > 1$. Therefore, in the following, we discuss the integrated yields $Y(n, x = 0 \ldots 3)$. The yields shown in Figures 2 and 3 are obtained from integrating the corresponding peaks in the mass spectra, and multiplying by the number of U atoms (i.e., n) in the cluster.

Figure 2b shows the effect of the detection efficiency correction on $Y(n)$. $Y(n)$ can be described by a power law $Y \sim n^{\delta}$ (the dotted and dashed lines in Figure 2b show fits of such a power law to the data) for $n > 1$. The ratio of corrected and uncorrected yields amounts to about 6.5 in the worst case ($n = 7$). As a consequence, the exponent δ is underestimated without correction for detection efficiency ($\delta = -3.2$). The corrected data yield a value of $\delta = -1.9$ in our example of Xe^{23+} (81 keV) impact

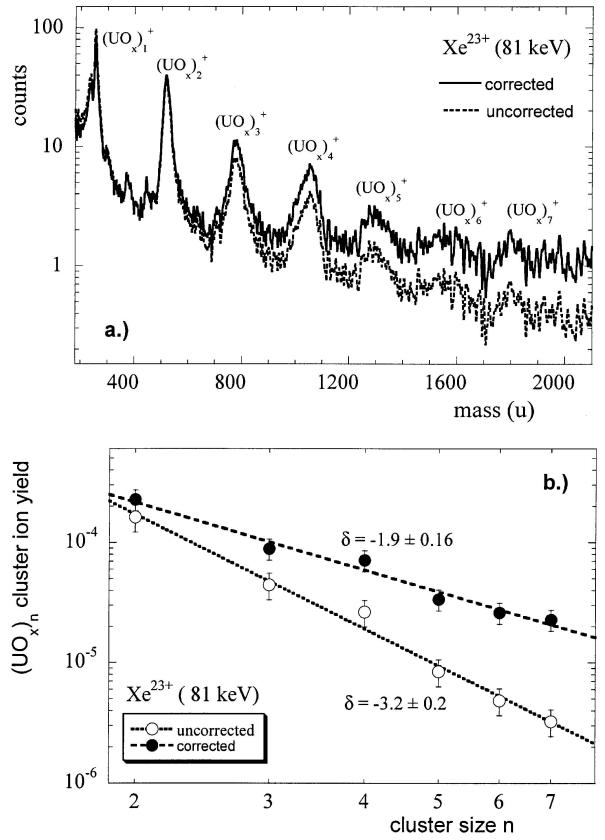

Fig. 2. (a) Mass-Spectrum (uncorrected as measured, and corrected for detection efficiency) of emitted positive secondary ions from an uranium dioxide target bombarded with Xe^{23+} ions at 81 keV at an incidence angle of 60° with respect to the surface normal. (b) Cluster size yield distributions from detection efficiency corrected and uncorrected mass spectra. The lines are fits of a power law $Y(n) \sim n^{\delta}$ to the data points.

on UO_2. The importance of the cluster-size dependent efficiency correction is thoroughly discussed by Staudt and Wucher [22]. Indeed, Figure 2b can be compared to Figure 11 of reference [22], where it is shown that δ changes from $\delta = -3.9$ to $\delta = -2.1$ for emission of In clusters by Xe^+ (15 keV) impact.

3 Cluster size distributions

Cluster size distributions as derived from time-of-flight mass spectra (compare Fig. 2) are shown in Figure 3. It is interesting to compare results obtained in the nuclear stopping regime to results obtained in the electronic stopping power regime. Therefore, first of all, distributions obtained with Kr^{32+} (11 MeV/u, $E_{kin} = 900$ MeV) in the electronic stopping regime by Schlutig et al. [15], measured with the time-of-flight mass spectrometer of Della Negra et al. [23] at GANIL-SME ("Sortie Moyenne Énergie"), are shown in Figure 3a. Data obtained by Hamza et al. with Th^{75+} ions at a kinetic energy of $E_{kin} = 83$ keV are shown in Figure 3b. These results can readily be compared to our new results obtained with Xe^{q+} ions of different charge states ($q = 10$ and 23, Fig. 3c), and Ne and Ar ($q = 8$, Fig. 3d) at comparable kinetic energy of $E_{kin} = 81$ keV. In all cases, the cluster-size distribution of the cluster ion yields $Y(n)$ can be described by a power law $Y \sim n^{\delta}$ for $n > 1$ with δ values between -1.5 and -3.

These findings are in contrast to "statistical models" (re-aggregation of individual atoms upon or after ejection), which predict exponential laws [12–15,22]. However, "collective ejection models" such as gas flow [12,15], thermodynamic (liquid-gas phase transition) [24], shock wave [25] indeed predict such power law dependencies [3]. The shock wave model yields [25] a value of $\delta = -2$, and the hydrodynamical (phase transition) model [24] predicts $\delta = -7/3$. These collective models could only be expected to be correct when a large number of atoms are set into movement by the deposited energy, i.e. for high sputter yields [12–15,22] (see Sect. 4). It comes therefore as a surprise to find a power law. Furthermore, it is surprising to find *high* δ values (around -2) also in the present case of relatively *low* sputter yields (around 4 uranium atoms per incoming projectile, see Fig. 4a). It is also remarkable that similar cluster-size distribution laws are observed in two projectile velocity regimes where the underlying physical mechanisms of sputtering are different.

Note that we excluded the monomers ($n = 1$) from the figures and the following discussion of the exponents δ. We observed that a fit of the power law $Y \sim n^{\delta}$ gave a significantly better correlation if only clusters with $n \geq 2$, and not the monomers $n = 1$ were taken into account. This interesting anomaly was also observed in previous studies of UO_2 sputtering by highly charged ions as can be seen from Figure 2 of Hamza et al. [13].

4 Correlation with the total sputtering yield

Hamza et al. [13] studied the emission of secondary ions from uranium dioxide with slow, highly charged ions such as Th^{75+} (Fig. 3b). They reported a correlation of the cluster size distribution with the *total sputter yield* Y_{tot}. They saw (see Fig. 3 of Ref. [13]) an increase from $\delta = -4$ to $\delta = -2.6$ when the total sputter yield is varied from $Y_{tot} \approx 15$ to $Y_{tot} \approx 90$. We also studied the total sputter yield Y_{tot} with xenon ions, always at fixed kinetic energy (81 keV), by means of a catcher technique [17,18]. The resulting total sputter yields [18] are shown in Figure 4a as a function of the potential energy E_{pot} of the ions (the charge states are indicated). A slight increase of the sputtering yield with the projectile charge state is observed. The main effect, a sputter yield of about $Y_{tot} \approx 4.2$, is connected to nuclear stopping. The charge state effect related to potential energy yields an additional sputtering of about one uranium atom per projectile for $E_{pot} \approx 9$ keV.

Let us plot the power law exponent δ as function of ion charge q (Fig. 4b) and as a function of the total sputter yield (Fig. 4c). For Ne and Ar the sputter yields were estimated from results of a SRIM [26] numerical simulation adjusted to the measured and calculated Xe data. The line drawn through the data points is to guide the eye.

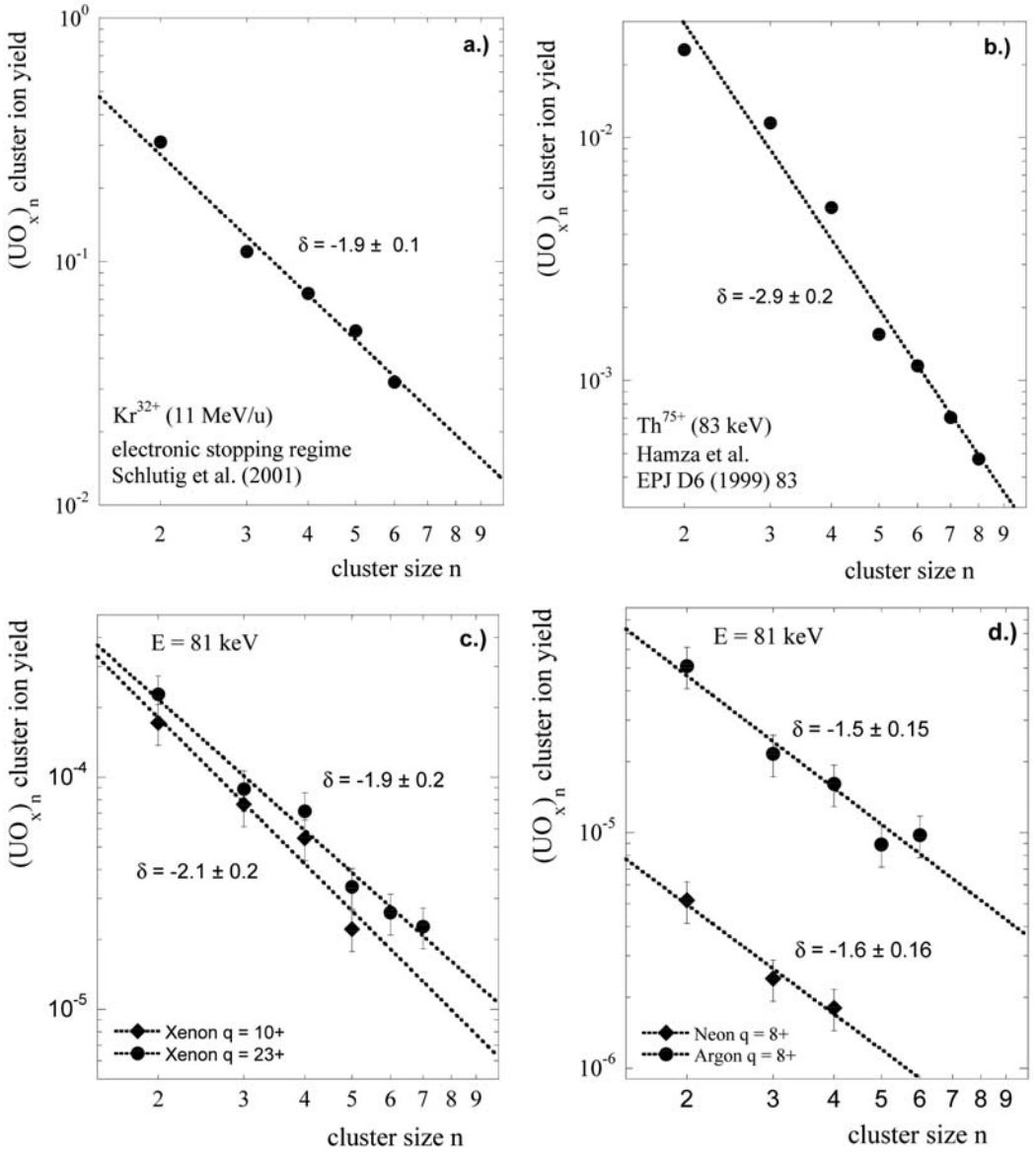

Fig. 3. The $(UO_x)_n$ cluster ion yield $Y(n)$ as a function of the cluster size n. The lines give a fit of a power law $Y \sim n^{\delta}$ to the data points. (a) High energy projectile (Kr^{32+}) at 11 MeV/u [15] (electronic sputtering). (b) Highly charged ions (Th^{75+}) at 83 keV from reference [13]. (c) Multicharged ions (Xe^{q+}, $q = 10, 23$) at 81 keV (this work). (d) Multicharged ions (Ar^{q+}, Ne^{q+}, $q = 8$) at 81 keV (this work).

We included the data point measured by Hamza et al. [13] with Th^{75+} at 83 keV. We observe that δ *decreases* with increasing total sputter yield Y_{tot} at fixed kinetic energy (Fig. 4b). No charge state effect can be seen for the xenon data, but a dependence on the projectile species (Ne, Ar, Xe), i.e. its mass, is observed.

This is surprising and at a first glance in contrast to the findings of Hamza et al. (Fig. 3 of Ref. [13]). However, these latter data were not taken at constant kinetic energy and mass of the projectiles so that different effects of different parameters may occur at the same time. It is also possible that specific effects occur with such heavy projectiles of extremely high charge states up to 75 connected to the fragmentation of excited clusters [2,12–14]. In-flight fragmentation of the clusters would lead to a lower δ value. It is conceivable that higher density of energy deposition leads to ejection of excited clusters with a limited lifetime.

It is also at a first glance difficult to understand why *high* δ values (around -2) are observed in the case of low sputter yields $Y_{tot} < 5$. Collective ejection models should be correct if a large number of target atoms are set into movement leading to a large number of ejected particles and high sputter yields. One may speculate that this finding is related to the statistical character of energy deposition. Most ion impacts only lead to a relatively low density of deposited energy. From time to time, however, there may be violent events leading to the ejection of many particles. A collective ejection model can then describe the underlying physical processes. There are indeed hints in the literature for such a statistical behavior with "mega-events" which contribute disproportionately to the average, mean total sputter yields [27]. This picture would also be in agreement with the finding that not every individual impact of a slow highly charged ion leads to the formation of a surface track [28].

It is possible to calculate the number of emitted U atoms per projectile impact event with the numerical simulation SRIM [26] in order to find a hint for the

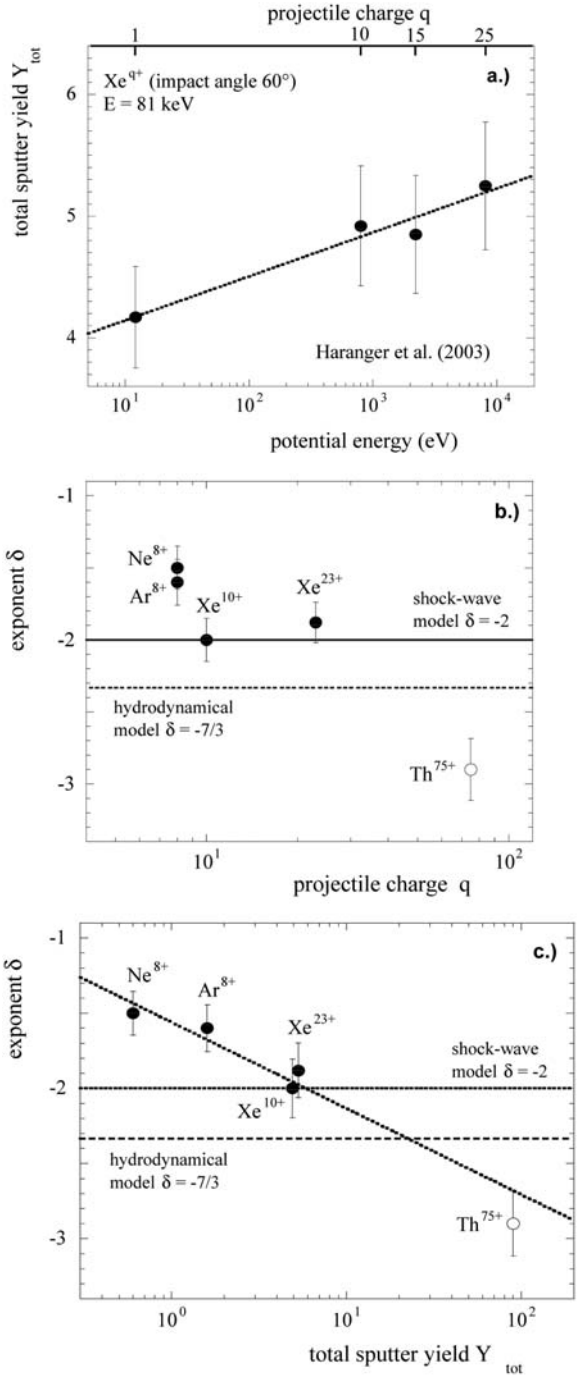

Fig. 4. (a) Total uranium sputter yield Y_{tot} as a function of the potential energy E_{pot} of xenon ions (the charge states are indicated). The impact angle is 60° with respect to the surface normal, the kinetic energy is 81 keV (from Refs. [17,18]). (b) The power law exponent δ (from Figs. 3c and 3d) as a function of the ion charge q. We included the data point measured by Hamza et al. [13] with Th^{75+} at 83 keV. The lines depict the values of δ predicted by the shock wave [25] model and the hydrodynamical [24] model. (c) Same as (b), but as a function of the total sputter yield. For Ne and Ar the sputter yields were estimated from results of a SRIM [26] numerical simulation adjusted to the measured and calculated Xe data. The line drawn through the data points is to guide the eye.

probability of "mega-events" We performed such a calculation for Xe projectiles at 81 keV. The distribution shows a maximum at about 2 emitted U atoms per projectile, with a smooth, rapid decay up to $n = 15$ emitted U atoms. In 65% of the events, $n = 0$ to 5 U atoms are emitted, in ≈20%, $n = 6$ to 10 and in ≈10%, $n = 11$ to 15. Randomly distributed events with emission of up to 35 U atoms are also observed. We can calculate the contribution of events with n emitted U atoms to the total sputter yield by multiplying the probability that n uranium atoms are emitted per projectile, $P(n)$, by the number of emitted U atoms, n. The result is that "big" events with $n > 15$ contribute by ≈15% of the total sputtering yield. We emphasize that SRIM calculations do not account for specific effects connected to high projectile potential energy, only collision cascades are accounted for. Furthermore, the cluster size distribution $Y(n)$ cannot be calculated directly.

5 Contribution of secondary ion monomer and cluster emission to sputtering

Another interesting result concerns the contribution of charged particle emission to the total sputter yield. Only a few studies exist which showed that most of the sputtered particles are ejected from the target as neutrals. Only a small fraction (ionization probabilities are of the order of 10^{-2} to 10^{-5}) is emitted as secondary ions [2,6]. As can be seen from Figures 3c and 3d, the measured yield of positively charged secondary ions containing uranium Y_{SI} increases strongly with the projectile mass: $Y_{SI} = (3 \pm 1) \times 10^{-5}$ for Ne^{8+}, $Y_{SI} = (4 \pm 0.9) \times 10^{-4}$ for Ar^{8+}, $Y_{SI} = (1.2 \pm 0.5) \times 10^{-3}$ for Xe^{10+} and $Y_{SI} = (1.9 \pm 0.7) \times 10^{-3}$ for Xe^{23+}, respectively. The yields were obtained from summing up the partial yields $Y(n)$, which were obtained by integrating the peaks for each n in the mass spectra and multiplying by the number of emitted U atoms n.

Thus, there is a charge state effect as in the case of the total sputter yields (Fig. 4a). If we compare the measured ionic yields to the measured total sputter yield of $Y_{tot} = 5$ (Fig. 4a), the contribution of SI is found to be approximately 3×10^{-4} for uranium dioxide bombarded by slow, multiply charged xenon ions. This is more than an order of magnitude lower than the fraction of secondary ions containing uranium observed by Schenkel et al. [6] for slow ions with charge states below $q = 30$, which is of the order of 5×10^{-3}. Schlutig et al. [15] estimate the contribution of positively charged secondary ions to the total sputtering to be approximately 10^{-2} in the high-energy electronic sputtering regime (Kr^{32+} at 11 MeV/u).

Finally, we note that the contribution of uranium emitted as ionic clusters $(UO_x)_n^+$ with $n \geq 2$ compared to emission as ionic monomer ($n = 1$) is quite important. The yield of ionic uranium clusters (i.e. the partial yields $Y(n)$ summed up over $n \geq 2$) is about 75% of the total yield of uranium emitted as secondary ions (i.e. the partial yields $Y(n)$ summed up over all n) for xenon, and about 80% for neon and argon projectiles. In other words,

the ratio of emitted ionic clusters to monomers varies from is 3 to 4.5 depending on the projectile. This is a further hint to support our speculation of violent "mega-events" occurring from time to time (every nth impact, with $n \gg 1$). Such events lead to the ejection of many particles and could favor the emission of clusters as compared to "smooth" events leading to no emission at all, or a very small sputtering yield [26].

6 Conclusion and outlook

Measurements of the cluster-size distribution were performed of positively charge secondary ions from sputtering of uranium dioxide UO_2 by neon and argon ions ($q = 8$) and xenon ions of different charge states ($q = 10, 23$) at fixed kinetic energy (81 keV). The size-distribution of the cluster ion yields Y can be described by a power law $Y \sim n^{\delta}$ with δ-values between -1.5 and -2.9. This is in agreement with the predictions of collective models. We also studied the correlation of the exponent δ with the total sputtering yield Y_{tot}. As a surprising result, a decrease was observed. It is at first glance astonishing that δ values around -2 are observed in the case of low sputter yields.

These findings together with the observed significant contribution of cluster ion emission to the total ion yield are an important hint for the statistical character of the energy deposition process. Most ion impacts only lead to relatively small density of deposited energy, but from time to time, violent "mega-events" which contribute disproportionately to the average, mean total sputter yields [27] can occur. For future experiments, it is promising to study *velocity and angular distributions* of emitted secondary ions by means of modern imaging techniques [29,30].

The experiments were performed at the LIMBE and SME beam lines of the "Grand Accélérateur National d'Ions Lourds" (GANIL) in Caen, France. Special thanks to J.-Y. Pacquet for his invaluable help in source tuning, and to F. Garrido for target preparation. T.J. acknowledges a EU post-doctoral grant from the HITRAP network, S.B. acknowledges a grant from the French-Algerian university exchange program, F.H. acknowledges a Ph.D. grant from CEA and the region of "Basse Normandie", A.R. acknowledges a EU Marie-Curie post-doctoral fellowship. We thank M. Toulemonde (Caen) and A. Meftah (Skikda) for making the stay of S.B. at CIRIL-Ganil possible.

References

1. *Fundamental Processes in Sputtering of Atoms and Molecules*, edited by P. Sigmund, K. Dan. Vid. Selsk. Mat. Fys. Medd. **43**, 1 (1993)
2. G. Betz, K. Wien, Int. J. Mass Spectrom. Ion Proc. **140**, 1 (1994)
3. R. Baragiola, Phil. Trans. R. Soc. Lond. A **362**, 29 (2004)
4. P. Sigmund, Phys. Rev. **184**, 383 (1969)
5. P. Sigmund, C. Clausen, J. Appl. Phys. **52**, 2 (1981)
6. T. Schenkel, A.V. Hamza, A.V. Barnes, D.H. Schneider, Progr. Surf. Sci. **61**, 23 (1999), and references therein
7. T. Neidhard, F. Pichler, F. Aumayr, Hp. Winter, M. Schmidt, P. Varga, Phys. Rev. Lett. **74**, 5280 (1995)
8. M. Toulemonde, W. Assmann, C. Trautmann, F. Grüner, H.D. Mieskes, H. Kucal, Z.G. Wang, Nucl. Instrum. Meth. B **212**, 346 (2003)
9. N. Itoh, T. Nakayama, Nucl. Instr. Meth. B **13**, 550 (1986)
10. F. Seitz, J.S. Koehler, in *Solid State Physics*, edited by F. Seitz, D. Turnbull (Academic Press, New York, 1956), Vol. 2, p. 307
11. R.L. Fleischer, P.B. Price, R.M. Walker, *Nuclear tracks in Solids: Principles and Applications* (University of California Press, Berkeley, 1975)
12. A. Wucher, M. Wahl, Nucl. Instrum. Meth. B **115**, 581 (1996)
13. A.V. Hamza, T. Schenkel, A.V. Barnes, Eur. Phys. J. D **6**, 83 (1999)
14. L.E. Rehn, R.C. Birtcher, S.E. Donnelly, P.M. Baldo, L. Funk, Phys. Rev. Lett. **87**, 207601 (2001)
15. S. Schlutig, thesis, University of Caen (2001)
16. S. Bouffard, J.P. Duraud, M. Mosbah, S. Schlutig, Nucl. Instrum. Meth. B **141**, 372 (1998)
17. F. Haranger, thesis, University of Caen (2003) (available from the authors on request)
18. B. Ban-d'Etat, F. Haranger, Ph. Boduch, S. Bouffard, H. Lebius, L. Maunoury, J.Y. Pacquet, H. Rothard, C. Clerc, F. Garrido, L. Thomé, R. Hellhammer, Z. Pešić, N. Stolterfoht, Phys. Scripta T **110**, 389 (2004)
19. L. Maunoury, R. Leroy, T. Been, G. Gaubert, L. Guillaume, D. Leclerc, A. Lepoutre, V. Mouton, J.Y. Pacquet, J.M. Ramillon, R. Vicquelin, the GANIL Ion Production Group, Rev. Sci. Instrum. **73**, 561 (2002)
20. M. Caron et al., Nucl. Instrum. Meth. B **146**, 126 (1998)
21. I.S. Gilmore, M.P. Seah, Int. J. Mass Spectrom. **202**, 217 (2000)
22. C. Staudt, A. Wucher, Phys. Rev. B **66**, 075419 (2002)
23. S. Della-Negra et al., J. Phys. France **48**, 261 (1987)
24. H.M. Urbassek, Nucl. Instrum. Meth. B **31**, 541 (1988)
25. I.S. Bitensky, E.S. Parilis, Nucl. Instrum. Meth. B **21**, 26 (1987)
26. `http://www.srim.org`, based on *The Stopping and Range of Ions in Solids*, edited by J.F. Ziegler, J.P. Biersack, U. Littmark (Pergamon Press, New York, 1985) (new edition in 2003)
27. M.H. Shapiro, T.A. Tombrello, Nucl. Instrum. Meth. B **152**, 221 (1999)
28. I.C. Gebeshuber, S. Cernusca, F. Aumayr, Hp. Winter, Nucl. Instrum. Meth. B **205**, 751 (2003)
29. T. Jalowy, Th. Weber, R. Dörner, L. Farenzena, V. Collado, E.F. Da Silveira, H. Schmidt-Böcking, K.O. Groeneveld, Int. J. Mass Spectrom. **231**, 51 (2004)
30. T. Jalowy, R. Neugebauer, M. Hattass, J. Fiol, F. Afaneh, J.A.M. Pereira, V. Collado, E.F. Da Silveira, H. Schmidt-Böcking, K.O. Groeneveld, Nucl. Instrum. Meth. B **193**, 762 (2002)